Journal of Ceramic Processing Research. Vol. 16, No. 2, pp. 232~236 (2015)

J O U R N A L O F
Ceramic Processing Research

Characteristics and electrochemical performance of the $LiMn_2O_4$ with TiO_2 surface layer in lithium secondary batteries

Cheon-Soo Kim[a,b], Keon Kim[b,*] and Cheol-Woo Yi[c,*]

[a]*Samsung SDI, 467 Beonyeong-ro, Seobuk-gu, Cheonan-si, Chungcheongnam-do 331-300, South Korea*
[b]*Department of Chemistry, Korea University, Seoul 136-701, South Korea*
[c]*Department of Chemistry and Institute of Basic Science, Sungshin Women's University, Seoul 136-742, South Korea*

To reduce high dissolution of manganese ions (Mn^{3+}) into the electrolytes in lithium-ion batteries, causing severe capacity loss during storage and cycle, TiO_2 is simply coated onto $LiMn_2O_4$ powders by the sol-gel method and investigated by various analytical techniques. Whereas the surface layer of TiO_2 on $LiMn_2O_4$ powders is stable up to 600 °C, annealing at and above 700 °C induces the reaction of TiO_2 surface layer with $LiMn_2O_4$ host particle. The passive TiO_2 layer on $LiMn_2O_4$ annealed at 500 °C effectively suppress Mn dissolution at room temperature and even higher temperature (55 °C). Moreover, TiO_2-coated $LiMn_2O_4$ annealed at 500 °C improves the cycle property at high voltage of 4.50 V charging and even at high temperature. Hence, TiO_2-coated $LiMn_2O_4$ can be a promising candidate of cathode active material for lithium-ion batteries.

Key words: $LiMn_2O_4$, TiO_2, Surface modification, Mn dissolution.

Introduction

The spinel $LiMn_2O_4$ as a cathode active material has been studied extensively in the field of large-scaled lithium-ion battery to be employed hybrid electric vehicles (PHEVs), electric vehicles (EVs), and energy storage systems (ESSs) since the report of the application of $LiMn_2O_4$ to a lithium secondary battery [1-5]. Even though $LiMn_2O_4$ has lower discharge capacity than $LiCoO_2$ used mainly in commvercial lithium-ion batteries for consumer electronics devices, it has many advantages such as lower cost, more safety, and less toxicity [1-5]. However, the spinel $LiMn_2O_4$ has a seriouss problem of irreversible capacity fading resulting in degradation of its performance. It is primarily originating from the dissolution of manganese ions (Mn^{3+}) into organic electrolyte [6, 7]. The capacity fading becomes significant especially at elevated temperatures [8], and it also causes relatively high self-discharge rate [9, 10], structure degradation during cycle [11] and Jahn-Teller distortion under over-discharge condition [12]. Much effort has been made to overcome the issue of capacity loss by doping cations [13] or anions [14], approaching various synthesis method of solid reaction [15-17], sol-gel reaction [18, 19], and Pechini process [20] and modifying the $LiMn_2O_4$ surface [21] to stabilize spinel structure and improve the cycle performance. The surface modification of the electrode active material is one of the effective methods to improve electrochemical properties while keeping the bulk properties.

In this paper, the surface of commercial $LiMn_2O_4$ is simply coated with TiO_2 using the sol-gel method to improve the electrochemical performance. The physico-chemical properties of 1 and 2 wt% TiO_2-coated $LiMn_2O_4$ annealed at 500-900 °C are examined. The electrochemical properties of the electrodes are investigated by various analytical techniques and the effect of TiO_2 surface layers on the cell performance is studied.

Experimental

Surface modification and coin-cell preparation

Commercial $LiMn_2O_4$ powder (Iljin Materials, Korea) is used as the host material for the surface modification and titanium butoxide (Aldrich, 98%, $Ti(O(CH_2)_3CH_3)_4$) is employed in a precursor for sol-gel reaction. Titanium butoxide is dissolved in methanol by stirring and followed by the addition of stoichiometric amounts of $LiMn_2O_4$ powder dispersed in methanol for 1 hour by stirring. This mixture is stirred for 5 hours at room temperature and then heated at 50 °C for 2 hours with stirring until it turned into a gel by solvent evaporation. Finally, the obtained gel precursor is calcined and sintered in an air atmosphere at various temperature (500-900 °C) for 5 hours with a fixed heating rate of 200 °C h^{-1} because the decomposition reaction is completed at ~ 500 °C based on TGA results about the gel precursor [19, 22].

The positive electrode is prepared with pristine or TiO_2-coated $LiMn_2O_4$ powders, carbon black (conductive agent), and poly(vinylidene fluoride) (PVdF; binder)

*Corresponding author:
Tel : +82-2-953-1172, 82-2-920-7666
Fax: +82-2-953-1172, 82-2-920-2047
E-mail: kkim@korea.ac.kr , cheolwoo@sungshin.ac.kr

with the weight ratio of 80, 10, and 10%, respectively. The slurry is prepared by mixing them in N-methyl-2-pyrrolidone (NMP) for 30 minutes using a planetary centrifugal mixer (SR-500, Thinky USA) and it was modified by a doctor-blade method on aluminum foil (substrate) as a current collector of positive electrode. Then, it was dried in a vacuum oven at 110 ºC overnight. The positive electrodes were pressed to obtain 80% of thickness prior to pressing and punched into a 10 mm diameter to fit a coin-cell. The coin cell (CR2032 type) is assembled in an Ar-filled glove box with the prepared positive electrode, lithium metal as negative electrode, polypropylene (PP) separator and electrolyte (Panaxetec, Korea). The electrolyte is 1.0 M $LiPF_6$ in a solvent mixture consisting of ethylene carbonate (EC) and diethyl carbonate (DEC) (1 : 1 v/v). This electrolyte is battery grade and used without any further treatment. This coin half-cell was kept at room temperature for ~ 20 hours to soak the electrolyte.

Characterization

The structure of prepared TiO_2-modified $LiMn_2O_4$ is characterized by x-ray diffraction (XRD; Bruker D8 Focus diffractometer equipped with a Cu target). The microstructure of the powder is observed by field emission scanning electron microscopy (FE-SEM, JSM-7500F, JEOL) and transmission electron microscopy (TEM, JEM-2100F, JEOL). The distribution of Ti is observed by energy dispersive spectroscopy (EDS, Horiba EX-200). To investigate the dissolution of Mn, the pristine and modified $LiMn_2O_4$ are immersed into the electrolyte at room temperature and the Mn concentration in the electrolyte is periodically measured by inductively coupled plasma-atomic emission spectroscopy (ICP-AES, Jobin Yvon 138 Ultrace). The electrochemical performances of the various compounds are evaluated using a WBCS 3000 instrument (WonA Tech., Korea). To investigate the cell performance, the batteries are charged at a 0.5 C-rate by constant current (CC) mode until its voltage reaches the pre-determined voltage from 4.30 or 4.50 V followed by constant voltage (CV) charging until the current declines to 0.05 C and then discharged at 0.5 C to cut-off voltage of 2.80 V.

Results and Discussion

Figure 1 shows XRD data of commercial spinel $LiMn_2O_4$ and 2 wt.% TiO_2-coated $LiMn_2O_4$ annealed at various temperatures (500-900 ºC). The XRD pattern of pristine $LiMn_2O_4$ indicates a typical spinel phases with (111), (311), (222), (400), (331), (511), (440) and (531) diffraction peaks (JCPDS: 88-1030) without any features related to impurities such as Li_2MnO_3, $LiMnO_2$ and/or MnO_2. To investigate the thermal behavior of TiO_2-coated $LiMn_2O_4$, XRD data are collected as a function of annealing temperature for 2 wt.% TiO_2-modified $LiMn_2O_4$. The TiO_2-coated $LiMn_2O_4$ annealed

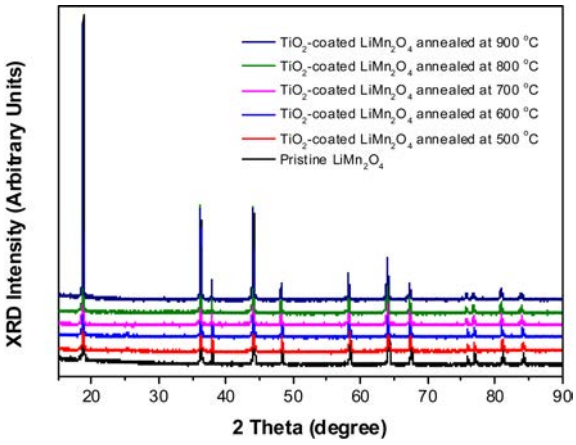

Fig. 1. XRD patterns of pristine $LiMn_2O_4$ and 2 wt% TiO_2-coated $LiMn_2O_4$ calcined at different annealing temperatures.

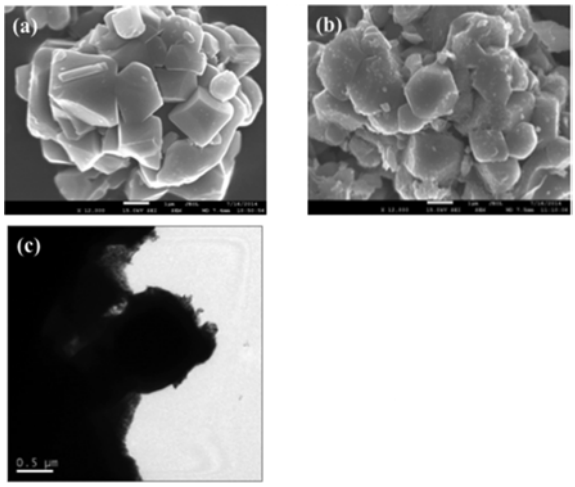

Fig. 2. SEM images of (a) pristine $LiMn_2O_4$ and (b) 2 wt.% TiO_2-coated $LiMn_2O_4$ annealed at different temperatures and (c) TEM image of 2 wt.% TiO_2-coated $LiMn_2O_4$ annealed at 500 ºC.

at 500 and 600 ºC shows a combination of x-ray scattering features consisting of anatase TiO_2 and spinel $LiMn_2O_4$ scattering features. The x-ray scattering feature at 25.3 º for the modified $LiMn_2O_4$ annealed at 500 and 600 ºC is the main scattering feature of anatase TiO_2 assigned (101) plane (JCPDS: 83-2243). Due to the addition of low concentration of titanium and overlapping with the features of host material ($LiMn_2O_4$), other scattering features assigned to the (004), (105), and (211) planes of anatase TiO_2 are not separately observed. However, the anatase TiO_2 scattering features of the peak at 25.3 º are diminished after annealing the sample at and above 700 ºC. It indicates that the reaction of TiO_2 and $LiMn_2O_4$ is not very favorable until 600 ºC and TiO_2 surface layer on $LiMn_2O_4$ is still stable up to that temperature. Even though previous studies [22, 23] reported that anatase TiO_2 phase in bulk or on ZnO transforms to rutile phase at and above 600 ºC, it is not observed in this study because the concentration of TiO_2 in this system is quite low. It is consistent with

the results from Chen *et al*. [21] and our previous report [22]. Chen *et al*. annealed TiO_2-coated $LiMn_2O_4$ at 700 °C and did not observe any other XRD features including TiO_2 except $LiMn_2O_4$ [21]. In addition, Hernan *et al*. [18] reported that Ti can dope the spinel $LiMn_2O_4$ by replacing Mn and retain the spinel structure. The annealing $LiMn_2O_4$ at and above 700 °C causes the disappearance of TiO_2 feature and it means Ti dopes into the host material by means of the reaction of Ti with $LiMn_2O_4$ at high temperature. The XRD data of pristine and TiO_2-coated $LiMn_2O_4$ even annealed at high temperature shown in Figure 1 are overlapped together throughout this experiment. It demonstrates that the original spinel structure is preserved and is a good agreement with previous studies [18, 21].

TiO_2-modified $LiMn_2O_4$ annealed at 500 °C is intensively studied since it is the lowest annealing temperature after calcination of gel precursor (lower processing cost by low heat treatment) and it is better temperature to get the simple coating effect without any doping effect. Figure 2 shows the morphologies of pristine and 2 wt.% TiO_2-modified $LiMn_2O_4$. The pristine $LiMn_2O_4$ has smooth surface and a typical spinel structure as shown in Figure 2 (a). However, the morphology of 2 wt.% TiO_2-modifzied $LiMn_2O_4$ annealed at 500 °C shows small particles on smooth surface of host particle as shown in Figure 2 (b). Figure 2 (c) is TEM image for 2 wt.% TiO_2-modified $LiMn_2O_4$ annealed at 500 °C and it confirms that the small particle completely covers $LiMn_2O_4$ particles. These small particles are TiO_2 formed by sol-gel reaction of titanium butoxide on $LiMn_2O_4$ host particles. It is good agreement with XRD data, as described in above, in that titania does not react with host particles but forms surface layer on the host particle by low temperature annealing (500-600 °C).

One of the most critical issues for using $LiMn_2O_4$ for a lithium ion battery is the dissolution of manganese ions (Mn^{3+}) into the $LiPF_6$-based electrolytes. The loss of active material by so-called 'Mn dissolution' induces the reduction of its capacity during storage and charge/discharge cycling. To investigate the effect of simple TiO_2 coating on Mn dissolution, the pristine and TiO_2-modified $LiMn_2O_4$ particles are immersed into the electrolyte at room temperature, and the concentration of Mn ions in the electrolyte is measured by ICP-AES. Figure 3 shows the concentrations of Mn ions for pristine and modified samples in the electrolyte as a function of immersion time. The concentration of Mn increases as an increase in the immersion time. After 30 days, the concentrations of Mn ions in the electrolyte are 880, 760, and 641 ppm for the pristine, 1 and 2 wt.% TiO_2-modified $LiMn_2O_4$ annealed at 500 °C, respectively. It is unambiguous that the concentration of Mn dissolved in the electrolyte is reduced as an increase in the amount of Ti coated onto $LiMn_2O_4$. It indicates that only the simple coating of TiO_2 onto the $LiMn_2O_4$ surface can effectively suppress the dissolution of manganese into

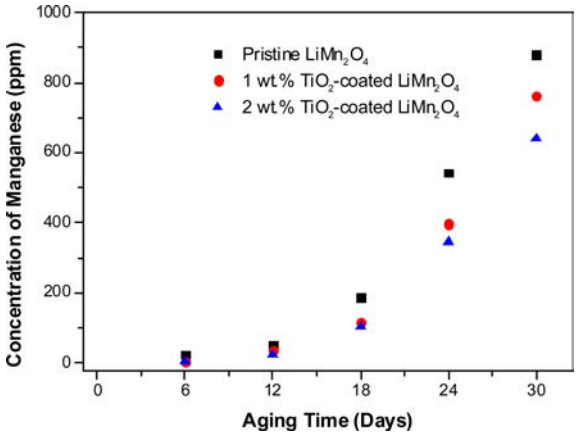

Fig. 3. Concentration of dissolved Mn in the electrolyte by ICP-AES for pristine $LiMn_2O_4$, 1 and 2 wt.% TiO_2-coated $LiMn_2O_4$ annealed at 500 °C.

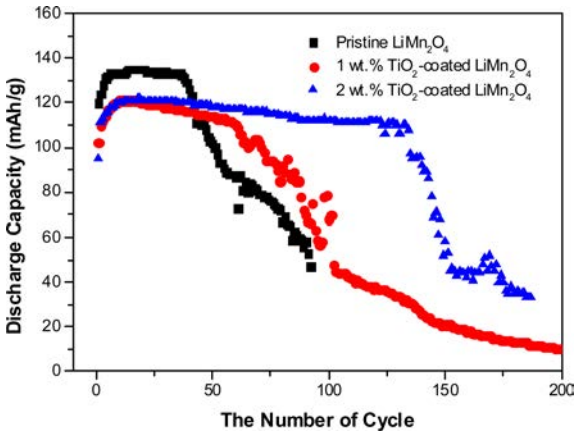

Fig. 4. Discharge capacities for charging voltage of 4.5 V at 55 °C of pristine $LiMn_2O_4$, 1 and 2 wt.% TiO_2-coated $LiMn_2O_4$ annealed at 500 °C.

the electrolyte because the surface titania can act as a protective layer against the dissolution of host material.

In order to identify the effect of the reduction of Mn dissolution on cycleability of the cell, charge/discharge cyclic experiments are performed with two-electrode batteries consisting of positive electrode prepared with pristine or modified $LiMn_2O_4$ annealed at 500 °C and lithium metal as negative electrode. Figure 4 shows the results of discharge capacities at 55 °C as a function of the number of cycle. The discharge capacity of pristine $LiMn_2O_4$ rapidly increases to 133 mAh g^{-1} at 10th cycle, keeps its capacity up to ~40th cycle, and then significantly decreases to ~47 mAh g^{-1} at 92nd cycle. This is the typical phenomenon in the cyclic experiments of $LiMn_2O_4$ battery due to capacity loss by structural degradation during cycle [11], especially, severe at elevated temperatures above 55 °C [8] and by high dissolution of manganese ions into the $LiPF_6$-based electrolytes [2, 6, 7, 17]. The initial discharge capacities of 1 and 2 wt.% TiO_2-modified $LiMn_2O_4$ has lower than that of pristine sample by ~15 mAh g^{-1} since the passive surface layer consisting of TiO_2 hinders the

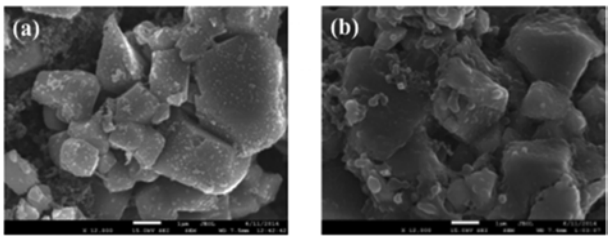

Fig. 5. SEM images of (a) pristine LiMn2O4 after 91 cycles of charge/discharge and (b) 2 wt. % TiO_2-coated $LiMn_2O_4$ annealed at 500 °C after 187 cycles of charge/discharge. Cycle is under the condition of charging voltage of 4.5 V at 55 °C.

transportation of Li ions during the charge-discharge process. However, it is clear that the cycleability of modified $LiMn_2O_4$ is improved in proportional to the amount of TiO_2 coated onto $LiMn_2O_4$. The drop points of retention capacity of the TiO_2-modified $LiMn_2O_4$ electrodes are significantly extended in comparison with that of the pristine $LiMn_2O_4$. The drop points of pristine $LiMn_2O_4$, 1 and 2 wt % TiO_2-modified $LiMn_2O_4$ are ~ 40, ~ 60 and > 120 cycles, respectively. Hence, life time of 1 and 2 wt % TiO_2-modified $LiMn_2O_4$ are improved by 150 and > 300% based on that of pristine $LiMn_2O_4$. It is good agreement with ICP-AES data as shown in Figure 3. The passive TiO_2 layer acts as a protective layer and it suppresses the dissolution of Mn into the electrolyte. Therefore, the cycleability of the modified $LiMn_2O_4$ is dramatically improved.

Figure 5 shows the morphology of pristine $LiMn_2O_4$ and 2 wt.% TiO_2-modified $LiMn_2O_4$ annealed at 500 °C after cyclic experiments under the condition of charging voltage of 4.50 V at 55 °C. $LiMn_2O_4$ electrode samples are disassembled from cell, washed by distilled water, rinsed by ethanol, and dried to get the SEM images after cycle. The initial morphology of the pristine $LiMn_2O_4$ is smooth surface in Figure 2 (a) but morphology after 91 cycles has many granules with a smooth surface as shown in Figure 5 (a). The formation of many granules is also one of the serious problems because the shape change of the $LiMn_2O_4$ electrode reduces the discharge capacity of the corresponding cells after 91 cycles. However, the morphology of the TiO_2-modified $LiMn_2O_4$ before and after cycles is quite different from that of the pristine $LiMn_2O_4$. In comparison with the initial morphology of 2 wt.% TiO_2-modified $LiMn_2O_4$ shown in Figure 2(b), the morphology after 187 cycles has a few granules with a smooth surface as shown in Figure 5(b). The morphology of modified $LiMn_2O_4$ after 187 cycles is not significantly different from its initial morphology.

Conclusions

High dissolution of manganese ions (Mn^{3+}) into the electrolytes is a critical problem of $LiMn_2O_4$ cathode and it causes capacity loss during storage and cycling. In order to overcome this drawback, TiO_2-coated $LiMn_2O_4$ was prepared by the sol-gel method and investigated by various analytical techniques. The TiO_2-modified $LiMn_2O_4$ annealed at 500-600 °C demonstrates that TiO_2 layer (anatase phase) is stable on the surface of $LiMn_2O_4$. However, the modified sample annealed at and above 700 °C shows the disappearance of anatase phase due to the reaction of TiO_2 surface layer with the host material ($LiMn_2O_4$) at high temperature. The TiO_2-modified $LiMn_2O_4$ annealed at 500 °C shows the improvement of electrochemical properties by suppressing the dissolution of manganese into the electrolyte, causing capacity loss. In addition, it effectively improves the cycle property at high voltage of 4.50 V charging and even at high temperature of 55 °C since the passive surface layer of TiO_2 prevents the transportation of Mn ions during storage and the charge-discharge process. Therefore, TiO_2 coating onto $LiMn_2O_4$ is a good treatment to improve its electrochemical properties and 2 wt.% TiO_2-modified $LiMn_2O_4$ annealed at 500 °C is a very promising candidate of cathode active material for lithium-ion batteries.

Acknowledgments

The author would like to acknowledge the help from colleagues at Korea University and Sungshin Women's University. The work was supported by the Sungshin Women's University Research Grant of 2014.

References

1. Y. Gao, J.R. Dahn, J. Electrochem. Soc., 143 (1996) 100-114.
2. O.K. Park, Y. Cho, S. Lee, H.C. Yoo, H.K. Song, J. Cho, Energy Environ. Sci., 4 (2011) 1621-1633.
3. J.M. Tarascon, D. Guyomard, J. Electrochem. Soc., 138 (1991) 2864-2868.
4. M.M. Thackeray, P.J. Johnson, L.A. Depicciotto, P.G. Bruce, J.B. Goodenough, Mater. Res. Bull., 19 (1984) 179-187.
5. M. Yoshio, R.J. Brodd, A. Kozawa, Lithium-Ion Batteries, Springer, 2009.
6. D.H. Jang, Y.J. Shin, S.M. Oh, J. Electrochem. Soc., 143 (1996) 2204-2211.
7. Y.Y. Xia, Y.H. Zhou, M. Yoshio, J. Electrochem. Soc., 144 (1997) 2593-2600.
8. Y.Y. Xia, N. Kumada, M. Yoshio, J. Power Sources, 90 (2000) 135-138.
9. H.T. Huang, C.A. Vincent, P.G. Bruce, J. Electrochem. Soc., 146 (1999) 481-485.
10. S.S. Zhang, M.S. Ding, T.R. Jow, J. Power Sources, 102 (2001) 16-20.
11. M.M. Thackeray, Y. Shao-Horn, A.J. Kahaian, K.D. Kepler, J.T. Vaughey, S.A. Hackney, Electrochem. Solid State Lett., 1 (1998) 7-9.
12. A. Yamada, M. Tanaka, Mater. Res. Bull., 30 (1995) 715-721.
13. G.H. Li, H. Ikuta, T. Uchida, M. Wakihara, J. Electrochem. Soc., 143 (1996) 178-182.
14. G.G. Amatucci, N. Pereira, T. Zheng, J.M. Tarascon, J.

Electrochem. Soc., 148 (2001) A171-A182.
15. Z. Kai, W. Yang, Z. Shuang, Y. Yan, P. Hao, L. Guiwei, J. Jianli, International journal of Electrochemical Science, 9 (2014) 5280-5288.
16. S.H. Park, S.W. Oh, S.T. Myung, Y.C. Kang, Y.K. Sun, Solid State Ion., 176 (2005) 481-486.
17. S.S. Zhang, T.R. Jow, J. Power Sources, 109 (2002) 172-177.
18. L. Hernan, J. Morales, L. Sanchez, J. Santos, Solid State Ion., 118 (1999) 179-185.
19. L. Hou, Y.D. Hou, M.K. Zhu, H.L. Tang, J.B. Liu, H. Wang, H. Yan, Mater. Lett., 59 (2005) 197-200.
20. W. Liu, G.C. Farrington, F. Chaput, B. Dunn, J. Electrochem. Soc., 143 (1996) 879-884.
21. L.H. Yu, X.P. Qiu, J.Y. Xi, W.T. Zhu, L.Q. Chen, Electrochim. Acta, 51 (2006) 6406-6411.
22. S.H. Lee, C.W. Yi, K. Kim, J. Phys. Chem. C, 115 (2011) 2572-2577.
23. P.S. Ha, H.J. Youn, H.S. Jung, K.S. Hong, Y.H. Park, K.H. Ko, J. Colloid Interface Sci., 223 (2000) 16-20.